

A method for estimating masses of W Ursae Majoris-type binaries

Li-Na Lu^{1,2}, Jin-Zhong Liu^{1,2}, Deng-Kai Jiang^{3,4} and Ya-Hui Wang⁵

¹ Xinjiang Astronomical Observatory, Chinese Academy of Sciences, Urumqi 830011, China; liujinzh@xao.ac.cn

² University of Chinese Academy of Sciences, Beijing 100049, China

³ Yunnan Observatories, Chinese Academy of Sciences, Kunming 650216, China

⁴ Key Laboratory for the Structure and Evolution of Celestial Objects, Chinese Academy of Sciences, Kunming 650216, China

⁵ Laboratory of New Energy and Materials, Xinjiang Institute of Engineering, Urumqi 830091, China

Received 2020 January 12; accepted 2020 May 30

Abstract Masses of W Ursae Majoris-type (W UMa) binaries play a critical role in investigating stellar dynamical evolutionary status. In this paper, we combine the PARSEC (PAdova and TRieste Stellar Evolution Code) with the Roche geometric model to provide a method to determine the masses of W UMa systems. To verify the validity of this method, we compile a sample of 140 spectrum binaries from the literature, which includes 76 W- and 64 A-subtype systems with reliable physical parameters. We find that the average fractional difference and the standard deviation (σM) of the residuals for W-subtype and A-subtype approximately amount to 15.66% and 0.1218, 16.03% and 0.2094, respectively. Meanwhile, we also perform detailed analyses in accordance with the orbital period, the effective temperatures and the mass ratio. We find that the method is more applicable to determine masses for W UMa systems with low effective temperature and short period.

Key words: stars: binaries: eclipsing — W Ursae Majoris (W UMa) binaries — masses

1 INTRODUCTION

W Ursae Majoris-type (W UMa) binaries are short-period binaries with spectral type from late A to middle K (Bilir et al. 2005). The W UMa binaries are known to be composed of main-sequence binaries for long time (Mochnacki 1981). The obvious character of W UMa binaries is that both components reach the inner Lagrangian point with a common convective envelope, which makes them with almost equal effective temperature (Yakut & Eggleton 2005). The previous works on W UMa systems have indicated that these systems exist some complicated physical courses, i.e., mass and energy transfer simultaneously between the components, angular momentum loss, periodic magnetic activity (Kähler 2002; Maceroni & van't Veer 1996; Borkovits et al. 2005). It is generally accepted that W UMa-type systems were classified as A- (massive-hotter stars) and W- (massive-cooler stars) subtype systems (Binnendijk 1970).

For eclipsing binaries, the absolute parameters can be determined from spectrum, radial velocity curves and light curves. Andersen (1991) reviews the errors for M and R less than 2%. However, the fundamental determinations of

masses and radii for 94 detached eclipsing binaries and alpha Centauri are with errors of $\pm 3\%$ accuracy or better (Torres et al. 2010). The mass of W UMa binaries can be determined accurately by the spectroscopic and photometric observations (e.g., Zola et al. 2010; Deb & Singh 2011; Zhu et al. 2013; Ma et al. 2018). Nevertheless, it is difficult to obtain both spectral and photometric observational results at the same time. We propose a method which can quickly and conveniently determine the masses of W UMa binaries with less observations and the stellar model. The method had been successfully applied by Wang et al. (2019) to determine the mass of AL Cas, and the detailed statistic and reliability analysis are presented in this paper. This could be a meaningful tool to fast estimate the masses of W UMa systems from large-scale surveys (e.g., identified by Jayasinghe et al. (2020) from All-Sky Automated Survey for Supernovae).

This paper is organized as follows. Section 2 describes the method in detail. Section 3 presents 140 W UMa-type systems as the reliable reference targets. In Section 4, we describe the results and illustrate the method with two examples. The discussions of our result are presented in

Section 5, and main conclusions are given in the last section.

2 METHOD

Combining PAdova TRieste Stellar Evolution Code (hereafter called: PARSEC) with the Roche model, we developed a method to determine the mass of W UMa systems. This method is mainly composed of two parts, as follows.

2.1 PARSEC Evolutionary Tracks

PARSEC code¹ was profoundly expended from Padova isochrones (Bertelli et al. 1994), which was updated by Bressan et al. (2012), Chevallard & Charlot (2016) and Fu et al. (2018). The pivotal updating includes equation of state, opacities, nuclear reaction rates, solar reference abundances as well as the addition of microscopic diffusion in low-mass stars, and so on.

In this paper, the star parameter space is obtained by PARSEC v1.2S stellar evolution code, and the input parameters are listed in Table 1. The parameter space mainly includes mass, metallicity (M/H), age (log Age), luminosity (log L), effective temperature (log T_e), surface gravity (log g), mass loss (M_{loss}), surface C/O ratios (C/O), nuclear reaction rates (M_{coreTP}), surface chemical abundances, the absolute magnitude of photometric system, and so on (Marigo et al. 2017). Tang et al. (2014) employed the relation $T - \tau$ from PHOENIX BT-Settl² atmospheres model to replace the grey atmosphere approximation $T - \tau$ relations $T^4(\tau) = \frac{3}{4}T_{\text{eff}}^4[\tau + q(\tau)]$ (Mihalas 1978) as the external boundary condition in PARSEC v1.2S stellar evolution code.

2.2 Roche Model

The Roche model was firstly proposed by Kuiper (1941), and it was based on two assumptions: (1) the masses of both companions were concentrated to the center; (2) the companions did not exist gravitational influence. In Cartesian coordinates, the formula of equipotential surfaces at any point (x, y, z) in space is given as (Mochnacki 1984):

$$\Psi(x, y, z) = -\frac{G(M_1 + M_2)}{2A}C, \quad (1)$$

where

$$C = \frac{2}{1+q} \frac{1}{(x^2 + y^2 + z^2)^{1/2}} + \left(x - \frac{q}{1+q}\right)^2 + y^2 \\ + \frac{2q}{1+q} \frac{1}{[(x-1)^2 + y^2 + z^2]^{1/2}}. \quad (2)$$

The effective radius of the Roche lobe is a major indicator of Roche lobe dimensions. It was derived by Paczyński (1971). Later, Eggleton (1983) modified the effective radius of Roche lobe as follows:

$$\frac{R_{\text{crl}}}{A} = \frac{0.49q^{2/3}}{0.6q^{2/3} + \ln(1 + q^{1/3})}, \quad 0 < q < \infty \quad (3)$$

where A stands for semi-major axis.

In this paper, we suppose that the radii of the companions are coincident with the effective radius of Roche lobe. According to Equation (3) and Kepler's third law, the mass-radius relation is derived as

$$\frac{R}{R_{\odot}} = \frac{2.0627p_{\text{orb}}^{2/3}q_*^{1/3}(q_* + 1)^{1/3}}{0.6q_*^{2/3} + \ln(1 + q_*^{1/3})} \left(\frac{M}{M_{\odot}}\right)^{1/3}, \quad (4)$$

where p_{orb} is the orbital period in day, and q_* defined as M_1/M_2 . Note that the more massive component is supposed as M_1 in this paper.

In our work, we obtain the stellar parameter space by PARSEC stellar evolution code with the input parameters listed in Table 1. Note that the radius of each star cannot be directly obtained by PARSEC model, so we use the formula $R = \sqrt{\frac{GM}{g}}$ to obtain the radius, where g and M are from the PARSEC stellar evolution code. Secondly, the effective temperature of the massive component with 400 K error is regarded as the condition to limit those parameter space. Thirdly, the above mass-radius relationship of Equation (4) is considered as the other to further constrain that space. Finally, the masses of targets can be determined by above two constraints to match out the star parameter space.

3 DATA

The absolute parameters of W UMa spectrum binaries were collected to verify the reliability of the method. These systems are sorted out based on the following criteria: (1) the spectroscopic and photometric observations of these systems have been carried out in previous research, (2) more than 15 spectra were observed, as well as (3) excluding the targets without error of mass ratio. Ultimately, the 140 W- and A-subtype systems are selected as reference targets, and the corresponding physical parameters are presented in Table 2. The input parameters of mass-radius relationship (Eq. (4)) are listed in the third and fourth column of Table 2. The effective temperature

¹ <http://stev.oapd.inaf.it/cgi-bin/cmd>

² PHOENIX is a general-purpose state-of-the-art stellar and planetary atmospheric code. This can calculate atmospheres and spectra of stars all across the Hertzsprung-Russel diagram including main sequence stars, giants, white dwarfs, stars with winds, TTauri stars, novae, supernova, brown dwarfs and extra solar giant planets. <http://perso.ens-lyon.fr/france.allard/index.html>

Table 1 Input Parameters of PARSEC

Name	Parameters	Reference
Mass	$0.1M_{\odot} < M < 350M_{\odot}$	[1]
Age	$6.6 < \log(t) < 10.13$	[1]
Metallicities	$0.0001 < Z < 0.07$	[1]
Evolutionary tracks	PARSEC version 1.2S	[1], [2]
Photometric system	<i>UBVRIJHK</i>	[3], [4], [5]
Circumstellar dust	No dust	[6]
Interstellar extinction	$R_v = 3.1, A_v = 0$	[7]

[1]: Chen et al. (2015); [2]: Chen et al. (2014); [3]: Maíz Apellániz (2006); [4]: Bessell (1990); [5]: Bessell & Brett (1988); [6]: Marigo et al. (2008), [7]: Girardi et al. (2008).

parameters of the massive components with 400 K error are regarded as the first condition to limit those parameters space, and are listed in the fifth column in this table. The mass parameters from the analysis of the radial-velocity and light curves are given in the seventh column.

4 RESULTS

In this paper, we utilize PARSEC V1.2S evolutionary tracks to obtain the grids of star parameter space with the initial input parameters in Table 1 for all reference targets. Based on the method in Section 2, the masses of more massive components of 140 W UMa systems are re-determined and listed in the sixth column of Table 2. The comparisons between our results and the subset from the literature are presented in Figure 1.

We calculate the average fractional difference ($\frac{1}{N} \sum_{i=1}^N \frac{|M_{\text{ref}} - M_{\text{model}}|}{M_{\text{ref}}}$) and the standard deviation (σM) of residuals ($\Delta M = M_{\text{ref}} - M_{\text{model}}$) in this section. The ΔM are listed in the eighth column of Table 2. For W- and A-subtype targets, the average fractional difference and the standard deviation (σM) of residuals amount to 15.66% and 0.1218, 16.03% and 0.2094, respectively. Figure 1 shows that our results are consistent with the mass parameters from literature for the low-mass targets. The BV Dra and TW Cet as samples are described in detail.

4.1 BV Draco

Based on the method described in Section 2, the mass and radius of BV Dra can be re-determined as $M_1 = 1.093 \pm 0.099M_{\odot}$ and $R_1 = 1.087 \pm 0.044R_{\odot}$, which is consistent with the result of Kaluzny & Rucinski (1986). For this target, Batten & Lu (1986) determined the mass ratio ($q = 0.411 \pm 0.006$) via seventy-two spectra obtained on four nights between February and April 1985 by 1.8-m telescope at Victoria. The photometric observations were updated by Yamasaki (1979); Geyer et al. (1982); Gorda (1986); Batten & Lu (1986); Dapergolas et al. (1989); Hardie & Hall (1990); Lee et al. (1999) and Yang et al. (2009a). Based on photoelectric

and spectroscopic observations, the absolute parameters of this system have been derived by Kaluzny & Rucinski (1986): $f = 76.280 \pm 0.32$, $M_1 = 1.040 \pm 0.020M_{\odot}$, $R_1 = 1.110 \pm 0.010R_{\odot}$, $M_2 = 0.430 \pm 0.010M_{\odot}$, $R_2 = 0.750 \pm 0.010R_{\odot}$, $T_1 = 6245$ K, $T_2 = 6345$ K.

A part of selected stars from PARSEC evolutionary tracks, with effective temperature in 5845 K to 6655 K, are shown on left side of Figure 2. The black solid lines in this figure originate from the mass-radius relationship described by Equation (4). As shown in this figure, the mass ($M_1 = 1.093 \pm 0.099M_{\odot}$) is determined by taking the average for the points surrounded by the black solid lines, which is consistent with the one ($M_1 = 1.040 \pm 0.020M_{\odot}$) from the literature.

4.2 TW Cetus

The procedure for TW Cet is same as for BV Dra. The mass ($M_1 = 0.959 \pm 0.092M_{\odot}$) of the massive component of TW Cet is determined by our method, and the value consistent with the one ($M_1 = 0.963 \pm 0.079M_{\odot}$) determined by Deb & Singh (2011). For TW Cet, the photometric observations were performed by Cillié & Bok (1951), Archer (1959) and Deb & Singh (2011). The spectroscopic observations of the target were carried out by Duerbeck & Rucinski (2007) and Naresh Kumar et al. (2008). According to the radial velocity curves from the 1.52m telescope of European Southern Observatory in 1996 and 1998, the genuine spectroscopic mass ratio is defined as 0.75 ± 0.03 (Duerbeck & Rucinski 2007). Combining the spectroscopic investigations with the photometric observations, the absolute parameters of TW Cet were achieved by Deb & Singh (2011), and these parameters are listed in Table 3.

The mass ($M_1 = 0.959 \pm 0.092M_{\odot}$) and radius ($R_1 = 0.939 \pm 0.072R_{\odot}$) of the massive component are determined in the right panel of Figure 2. It is obvious that the computed value is consistent with the one of the literature. The comparisons of two samples between the reference masses and the values derived by our method are listed in Table 3. Meanwhile, note that we use the value of $A_v = 0$ as an input parameter in the current study. Because we find the maximum fractional difference ($\frac{\text{Mass}_{A_v=0} - \text{Mass}_{A_v \neq 0}}{\text{Mass}_{A_v=0}}$) for all sets of parameters is 2.4%.

5 DISCUSSION

As displayed in Section 4, our results are in good agreement with those from the literature for low-mass companions stars. However, we also find obvious discrepancy for the massive component, regardless the subtypes of the targets. Therefore, we perform the following detailed

Table 2 The Main Physical Parameters for Contact Binary Systems

Star	Subtype	Input parameters			M_{Model} (M_{\odot})	M_{ref} (M_{\odot})	ΔM (M_{\odot})	Ref
		P_{orb}^{α} (day)	q^{α}	T (K)				
V829 Her	W	0.358	0.408 (008)	6300	1.056(127)	1.300 (030)	0.244(130)	[1]
V417 Aql	W	0.370	0.362 (007)	5860	1.019(145)	1.377 (036)	0.358(149)	[2]
VZ Lib	W	0.358	0.330 (040)	5770	1.085(128)	1.060 (060)	-0.024(142)	[3], [4]
AB And	W	0.332	0.560 (007)	5140	1.120(132)	1.042 (006)	-0.078(138)	[5], [6]
AD Phe	W	0.380	0.370 (010)	5717	1.071(118)	1.179 (157)	0.108(196)	[7]
RW Dor	W	0.285	0.630 (003)	5272	0.890(061)	0.830 (128)	-0.060(142)	[7]
TX Cnc	W	0.389	0.455 (011)	6121	1.182(112)	1.322 (044)	0.163(127)	[7]
V2377 Oph	W	0.425	0.395 (012)	5418	1.023(065)	1.038 (192)	0.015(202)	[7]
NSVS 254037	W	0.318	0.410 (009)	5585	0.996(087)	1.150 (007)	0.153(087)	[8]
V2162 Oph	W	0.375	0.286 (003)	6250	1.176(162)	1.300 (100)	0.124(191)	[9]
V1128 Tau	W	0.305	0.534 (006)	6200	0.939(079)	1.000 (006)	0.161(049)	[9]
AM Leo	W	0.366	0.440 (010)	5942	1.063(101)	1.230 (080)	0.167(128)	[10]
BB Peg	W	0.362	0.363 (020)	5905	1.091(128)	1.420 (040)	0.328(134)	[11]
UX Eri	W	0.445	0.373 (021)	6100	1.245(155)	1.430 (030)	0.184(157)	[12]
GR Vir	W	0.347	0.122 (044)	6150	1.180(158)	1.376 (026)	0.195(160)	[12]
AH Aur	W	0.494	0.169 (059)	6200	1.124(186)	1.674 (048)	0.549(192)	[12]
YY Crb	W	0.377	0.243 (008)	6100	1.162(121)	1.393 (025)	0.231(123)	[12]
EF Boo	W	0.421	0.512 (008)	6450	1.168(129)	1.547 (035)	0.379(133)	[12]
V410 Aur	W	0.366	0.144 (013)	5890	1.109(103)	1.270 (061)	0.161(119)	[13]
CK Boo	W	0.355	0.111 (052)	6150	1.166(168)	1.442 (024)	0.276(169)	[13]
VY Sex	W	0.443	0.313 (005)	5756	1.050(077)	1.423 (016)	0.373(078)	[13]
AQ Psc	W	0.476	0.226 (002)	6100	0.980(168)	1.682 (032)	0.702(171)	[13]
FP Boo	W	0.641	0.106 (005)	6980	1.550(244)	1.614 (052)	0.064(250)	[13]
V2357 Oph	W	0.416	0.231 (010)	5640	1.041(124)	1.191 (012)	0.150(124)	[13]
FU Dra	W	0.307	0.251 (030)	5670	1.033(039)	1.173 (023)	0.140(045)	[14]
UV Lyn	W	0.415	0.367 (007)	5770	1.062(152)	1.344 (025)	0.282(154)	[14]
HT Vir	W	0.408	0.702 (014)	6010	1.138(120)	1.284 (015)	0.145(120)	[14]
OU Ser	W	0.297	0.173 (017)	5950	1.064(119)	1.109 (038)	0.045(125)	[14]
BX Dra	W	0.579	0.289 (016)	7000	1.498(263)	2.194 (132)	0.696(294)	[15]
RT LMi	W	0.375	0.366 (038)	6200	1.110(150)	1.307 (046)	0.196(156)	[15]
V842 Her	W	0.419	0.259 (024)	5326	1.031(064)	1.455 (026)	0.424(069)	[16]
V502 Oph	W	0.455	0.335 (009)	5900	1.097(162)	1.370 (020)	0.273(163)	[17]
V345 Gem	W	0.275	0.142 (003)	6115	1.040(076)	1.050 (050)	0.010(090)	[18]
XY Leo	W	0.284	0.729 (007)	4524	0.819(002)	0.820 (090)	0.001(009)	[19]
GZ And	W	0.305	0.514 (008)	5021	0.946(055)	1.250 (040)	0.304(068)	[20]
V753 Mon	W	0.677	0.970 (009)	7728	1.756(270)	1.647 (000)	-0.109(270)	[21]
PY Boo	W	0.311	0.773 (005)	4850	0.949(055)	1.011 (003)	0.061(055)	[22]
AP Leo	W	0.430	0.297 (009)	6150	1.256(149)	1.470 (000)	0.214(149)	[23]
TZ Boo	W	0.297	0.207 (005)	5890	1.030(104)	0.990 (030)	-0.040(108)	[24]
FG Hya	W	0.328	0.112 (004)	5900	1.113(207)	1.080 (000)	-0.033(207)	[25]
RW Com	W	0.237	0.471 (006)	4720	0.814(048)	0.800 (020)	-0.013(052)	[26]
BD+07°3142	W	0.275	0.852(004)	4640	0.662 (008)	0.740 (050)	-0.111(064)	[26]
SS Ari	W	0.406	0.313 (003)	5860	1.235(004)	1.310 (000)	0.075(034)	[27]
TY Boo	W	0.317	0.437 (007)	5800	1.019(090)	0.930 (020)	-0.089(093)	[28]
V757 Cen	W	0.343	0.701 (020)	5900	1.022(101)	0.880 (090)	-0.142(135)	[29]
VW Cep	W	0.278	0.302 (070)	5050	0.913(045)	1.130 (000)	0.217(045)	[30]
BW Dra	W	0.292	0.280 (005)	5980	0.955(112)	0.920 (020)	-0.035(114)	[31]
V728 Her	W	0.471	0.181 (022)	6622	1.412(217)	1.650 (000)	0.238(217)	[32]
V781 Tau	W	0.345	0.393 (046)	5621	1.069(094)	1.240 (029)	0.171(098)	[33]
RZ Com	W	0.339	0.430 (030)	6165	1.011(138)	1.230 (000)	0.219(138)	[34], [35]
V2612 Oph	W	0.375	0.286 (011)	6250	1.176(162)	1.300 (040)	0.171(158)	[9]
AE Phe	W	0.3624	0.16 (040)	5888	1.185(129)	1.380(000)	0.195(129)	[57]
ET Leo	A	0.347	0.342 (005)	5500	1.163(092)	1.586 (021)	0.423(094)	[13]
XZ Leo	A	0.488	0.348 (029)	7240	1.469(196)	1.742 (047)	0.272(201)	[13]
V839 Oph	A	0.409	0.305 (024)	6650	1.187(182)	1.572 (031)	0.385(184)	[13]
V921 Her	A	0.877	0.226 (005)	7700	1.562(385)	2.068 (049)	0.506(361)	[13]
XX Sex	A	0.5401	0.773 (050)	6881	1.356(272)	1.301 (022)	-0.055(273)	[7]
EQ Tau	A	0.341	0.442 (007)	5860	1.056(106)	1.233 (030)	0.177(110)	[14]
HN UMa	A	0.383	0.145 (002)	6100	1.027(164)	1.279 (060)	0.252(174)	[14]
CN And	A	0.463	0.390 (033)	6450	1.03(156)	1.132 (036)	0.028(160)	[14], [81]
V592 Per	A	0.716	0.408 (008)	6800	1.430(254)	1.743 (056)	0.313(260)	[14]
V376 And	A	0.799	0.516 (007)	8350	1.984(321)	2.491 (057)	0.507(326)	[15]
UZ Leo	A	0.618	0.303 (024)	6980	1.477(249)	1.989 (039)	0.512(252)	[15]
EX Leo	A	0.409	0.199 (036)	6340	1.174(184)	1.573 (034)	0.399(187)	[15]
V523 Cas	A	0.234	0.516 (007)	4500	0.716(010)	0.740 (001)	0.024(010)	[15]

Table 2 *Continued.*

Star	Subtype	Input parameters			Masses of primary stars from this method	Masses of primary stars from the literature	ΔM (M_{\odot})	Ref
		P_{orb}^{α} (day)	q^{α}	T (K)	M_{Model} (M_{\odot})	M_{ref} (M_{\odot})		
EE Cet	A	0.341	0.315(050)	6314	1.025(148)	1.370(000)	0.354(148)	[19]
QX And	A	0.412	0.396(009)	6440	1.111(175)	1.470(005)	0.359(175)	[26]
AK Her	A	0.422	0.277(024)	6500	1.174(022)	1.200(200)	0.026(201)	[9]
HI Dra	A	0.597	0.250(050)	7000	1.564(259)	1.700(300)	0.136(396)	[9]
DX Tuc	A	0.377	0.290(040)	6250	1.118(167)	1.000(030)	-0.118(169)	[4]
AU Ser	A	0.387	0.710(020)	5495	1.068(091)	0.895(100)	-0.173(091)	[36]
DK Cyg	A	0.471	0.307(008)	7500	1.374(292)	1.820(070)	0.445(300)	[37]
GM Dra	A	0.339	0.180(007)	6450	1.109(129)	1.213(041)	0.119(135)	[19]
EF Dra	A	0.424	0.160(014)	6250	1.309(145)	1.815(032)	0.506(148)	[38]
HV Aqr	A	0.375	0.145(050)	6460	1.224(171)	1.355(001)	0.131(171)	[39]
DZ Psc	A	0.366	0.136(010)	6210	1.211(063)	1.352(057)	0.141(084)	[12]
OO Aql	A	0.507	0.846(007)	6100	1.161(188)	1.060(007)	-0.100(188)	[40]
TW Cet	A	0.317	0.750(030)	5865	0.959(092)	0.963(097)	0.004(133)	[41]
DY Cet	A	0.441	0.356(009)	6650	1.218(183)	1.436(034)	0.217(186)	[41]
TY Pup	A	0.819	0.250(030)	6881	1.353(425)	1.422(205)	0.069(472)	[41]
HI Pup	A	0.433	0.190(060)	6662	1.378(182)	1.245(270)	-0.132(325)	[41]
VW Boo	A	0.3423	0.428(030)	5560	1.051(094)	1.084(070)	0.033(094)	[53]
V868 Mon	A	0.638	0.373(008)	7000	1.432(288)	2.117(032)	0.685(289)	[41]
XX Sex	A	0.540	0.773(005)	6881	1.377(196)	1.301(022)	-0.076(197)	[41]
AG Vir	A	0.643	0.382(021)	8180	1.798(295)	2.139(024)	0.340(295)	[41]
MW Pav	A	0.795	0.915(012)	6881	1.479(275)	1.520(045)	0.040(278)	[41]
V357 Peg	A	0.579	0.401(004)	7000	1.492(284)	1.720(015)	0.227(284)	[41]
EL Aqr	A	0.484	0.203(008)	6881	1.355(263)	1.655(070)	0.300(272)	[41]
XY Boo	A	0.371	0.160(040)	6324	1.228(168)	0.912(280)	-0.315(326)	[42]
ϵ s CrA	A	0.591	0.128(014)	7100	1.538(298)	1.720(040)	0.181(300)	[43]
V401 Cyg	A	0.583	0.290(011)	6700	1.458(289)	1.680(000)	0.221(289)	[44]
V1073 Cyg	A	0.786	0.317(070)	6700	1.414(360)	1.600(020)	0.186(306)	[45]
TV Mus	A	0.446	0.120(010)	6088	1.188(017)	0.940(140)	-0.248(220)	[46]
V508 Oph	A	0.345	0.520(006)	6000	1.043(108)	1.010(000)	-0.032(108)	[47]
V566 Oph	A	0.410	0.263(012)	7000	1.132(198)	1.400(000)	0.268(198)	[48]
Y Sex	A	0.420	0.180(030)	6210	1.242(204)	1.210(000)	-0.032(204)	[49]
RZ Tau	A	0.416	0.369(001)	7300	1.255(136)	1.700(160)	0.445(209)	[50]
AW UMa	A	0.439	0.078(080)	7175	1.605(201)	1.790(140)	0.185(245)	[51]
SX Crv	A	0.317	0.066(003)	6340	1.173(193)	1.246(040)	0.072(197)	[3]
U Peg	A	0.375	0.331(001)	5860	1.237(043)	1.149(009)	-0.088(043)	[52]
VW Boo	A	0.342	0.428(003)	5560	1.035(107)	1.084(007)	0.049(107)	[53]
PY Vir	A	0.311	0.773(005)	4830	0.899(028)	0.950(010)	0.050(280)	[54]
CC Com	A	0.221	0.526(010)	4300	0.708(036)	0.717(014)	0.009(038)	[55]
AO Cam	A	0.330	0.413(010)	5900	1.038(080)	1.119(007)	0.080(099)	[5]
VZ Psc	A	0.261	0.800(014)	4500	0.726(009)	0.651(026)	-0.075(093)	[74]
SW Lyn	W	0.441	0.520(030)	6700	1.199(161)	1.716(050)	0.517(168)	[58], [83]
QW Gem	W	0.358	0.334(009)	6100	1.081(159)	1.314(035)	0.233(163)	[58], [83]
V2150 Cyg	A	0.592	0.802(060)	7920	2.35(338)	1.644(253)	0.7056(422)	[58], [82]
ND Cam	W	0.498	0.421(060)	6700	1.309(239)	1.849(021)	0.541(239)	[5], [82]
UX Eri	A	0.421	0.512(008)	6100	1.430(030)	1.143(131)	0.286(134)	[12], [83]
SW Lac	W	0.321	0.777(010)	5800	1.240(024)	0.921(110)	0.319(113)	[12]
GR Vir	A	0.321	0.122(044)	6450	1.376(026)	1.121(146)	0.254(148)	[12]
NN Vir	A	0.481	0.490(011)	6925	1.730(024)	1.287(146)	0.443(195)	[12]
V776 Cas	A	0.440	0.130(004)	6700	1.750(040)	1.362(387)	0.387(264)	[14]
UV Lyn	W	0.307	0.367(070)	6500	1.344(025)	0.991(0870)	0.353(090)	[14]
HT Vir	A	0.408	0.900(040)	6500	1.284(015)	1.067(153)	0.217(153)	[14]
XZ Leo	A	0.488	0.348(029)	7240	1.469(196)	1.742(047)	0.272(201)	[13]
VY Sex	W	0.443	0.313(005)	6756	1.266(213)	1.423(016)	0.157(213)	[13]
UZ Leo	W	0.618	0.303(024)	6980	1.527(268)	1.989(036)	0.462(270)	[15]
AM Leo	W	0.366	0.459(040)	6100	1.089(131)	1.294(014)	0.205(132)	[15]
EX Leo	W	0.409	0.199(036)	6340	1.187(190)	1.573(034)	0.386(193)	[15]
RT Lmi	W	0.375	0.366(038)	6200	1.116(154)	1.307(046)	0.191(161)	[15]
BH Cas	A	0.406	0.474(002)	4790	0.850(060)	0.921(191)	0.059(230)	[59], [82]
V523 Gas	W	0.234	0.516(080)	4434	0.727(095)	0.637(000)	-0.089(094)	[60], [61], [82]
ER Ori	W	0.423	0.502(040)	5800	1.117(131)	1.385(000)	0.268(131)	[60], [62], [81]
FN Cam	W	0.677	0.222(005)	6700	1.609(380)	2.400(006)	0.791(379)	[63], [81]
S Ant	A	0.648	0.590(020)	7800	1.630(314)	1.784(258)	0.121(258)	[60], [62], [81]
AA Uma	W	0.468	0.549(014)	5873	1.104(230)	1.610(030)	0.506(049)	[64], [81]
HT Vir	A	0.408	0.812(008)	6100	1.133(125)	1.284(015)	0.151(125)	[14], [65]
FI Boo	W	0.390	0.373(060)	5420	1.059(095)	1.070(060)	0.065(112)	[66]

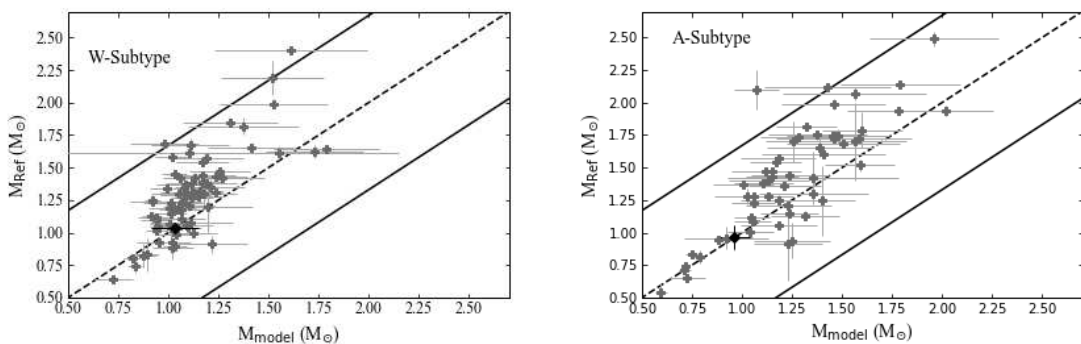
Table 2 *Continued.*

Star	Subtype	Input parameters			Masses of primary stars from this method	Masses of primary stars from the literature	ΔM (M_\odot)	Ref
		P_{orb}^α (day)	q^α	T (K)	M_{Model} (M_\odot)	M_{ref} (M_\odot)		
V535 Ara	A	0.629	0.319(020)	8200	1.874(240)	1.940(040)	0.065(243)	[67]
NSVS 4161544	W	0.352	0.296(005)	5726	1.108(139)	1.285(006)	0.365(139)	[68]
SDSS J001641-00425	A	0.198	0.620(010)	4342	0.591(031)	0.680(030)	-0.050(078)	[69]
J093010B	A	0.230	0.397(006)	5185	0.792(055)	0.832(018)	0.044(055)	[70]
V972 Her	W	0.443	0.163(088)	6046	1.215(181)	0.910(070)	-0.305(194)	[71]
V351 Peg	W	0.593	0.360(020)	7559	1.728(242)	1.627(050)	-0.101(247)	[72], [73]
BI CVn	W	0.384	0.410(027)	6700	1.111(134)	1.280(024)	0.141(136)	[75], [80]
DU Boo	A	1.056	0.234(035)	7850	1.799(321)	2.080(020)	0.281(333)	[76], [80]
GW Cnc	W	0.281	0.265(007)	6790	0.957(067)	0.971(016)	0.013(068)	[77], [80]
HH Boo	W	0.319	0.588(004)	5680	1.007(058)	1.068(045)	0.059(073)	[78], [80]
V1191 Cyg	W	0.313	0.110(027)	6215	1.086(131)	1.280(020)	0.194(132)	[79], [80]

α represents input parameter of mass-radius relationship of Equation (4). T represents the effective temperature parameters of the massive component, and $T \pm 400$ K is regarded as the first condition to limit those parameters space. q is defined as M_2/M_1 , from observations. ΔM is defined as $M_{\text{ref}} - M_{\text{model}}$. M_{ref} represents the reference masses from the analysis of the radial-velocity and light curves. Ref. [1]: Erdem & Özkardeş (2006); [2]: Lu & Rucinski (1999); [3]: Zola et al. (2004); [4]: Szalai et al. (2007); [5]: Baran et al. (2004); [6]: Pych et al. (2004); [7]: Deb & Singh (2011); [8]: Kjurkchieva et al. (2018); [9]: Çalışkan et al. (2014); [10]: Gorda (2016); [11]: Kalomeni et al. (2007); [12]: Gazeas et al. (2005); [13]: Gazeas et al. (2006); [14]: Zola et al. (2005); [15]: Zola et al. (2010); [16]: Selam et al. (2005); [17]: Xiao et al. (2016); [18]: Yang et al. (2009b); [19]: Djurašević et al. (2006); [20]: Yang & Liu (2003a), [21]: Qian et al. (2013); [22]: Kjurkchieva et al. (2019a); [23]: Lu & Rucinski (1999); [24]: Christopoulou et al. (2011); [25]: Qian & Yang (2005); [26]: Djurašević et al. (2011); [27]: Kim et al. (2003); [28]: Rainger et al. (1990); [29]: Kaluzny (1984); [30]: Mitnyan et al. (2018); [31]: Kaluzny & Rucinski (1986); [32]: Nelson et al. (1995); [33]: Lu (1993); [34]: Nelson & Alton (2019); [35]: Hilditch et al. (1988); [36]: Gürol (2005); [37]: Lee et al. (2015); [38]: Yang (2012); [39]: Li & Qian (2013); [40]: Li et al. (2016); [41]: Deb & Singh (2011); [42]: Yang et al. (2005); [43]: Goecking & Duerbeck (1993); [44]: Rucinski et al. (2002); [45]: Ahn et al. (1992); [46]: Hilditch et al. (1989); [47]: Lapasset & Gomez (1990); [48]: Niarchos & Manimanis (2003); [49]: Yang & Liu (2003b); [50]: Yang & Liu (2003c); [51]: Pribulla et al. (1999); [52]: Pribulla & Vanko (2002); [53]: Liu et al. (2011); [54]: Zhu et al. (2013); [55]: Köse et al. (2011); [56]: Ma et al. (2018); [57]: Barnes et al. (2004); [58]: Kreiner et al. (2003); [59]: Liu et al. (2019); [60]: Bilir et al. (2005); [61]: Lister et al. (2000); [62]: Russo et al. (1982); [63]: Pribulla et al. (2002); [64]: Lee et al. (2011); [65]: Lu et al. (2001); [66]: Papageorgiou & Christopoulou (2014); [67]: Özkardeş & Erdem (2012); [68]: Kjurkchieva et al. (2019b); [69]: Davenport et al. (2013); [70]: Lohr et al. (2015); [71]: Selam et al. (2018); [72]: Albayrak et al. (2005); [73]: Rucinski et al. (2001); [74]: Ma et al. (2018); [75]: Qian et al. (2008); [76]: Djurašević et al. (2013); [77]: Gürol et al. (2016); [78]: Gürol et al. (2015); [79]: Gürol (2016); [80]: Kouzuma (2019); [81]: Csizmadia & Klagyivik (2004); [82]: Liu et al. (2018); [83]: Bilir et al. (2005).

Table 3 Parameter Comparison of BV Dra and TW Cet

Parameters	BV Dra	Reference	TW Cet	Reference
P_{orb}	0.350 d	Kaluzny & Rucinski (1986)	0.317 d	Duerbeck & Rucinski (2007)
q	0.411 ± 0.006	Kaluzny & Rucinski (1986)	0.750 ± 0.030	Duerbeck & Rucinski (2007)
T	6245 K	Kaluzny & Rucinski (1986)	5865 K	Deb & Singh (2011)
M_{ref}	$1.040 \pm 0.020 M_\odot$	Kaluzny & Rucinski (1986)	$0.963 \pm 0.079 M_\odot$	Deb & Singh (2011)
R_{ref}	$1.110 \pm 0.010 R_\odot$	Kaluzny & Rucinski (1986)	$0.950 \pm 0.013 R_\odot$	Deb & Singh (2011)
M_{model}	$1.093 \pm 0.099 M_\odot$	this paper	$0.959 \pm 0.092 M_\odot$	this paper
R_{model}	$1.087 \pm 0.044 R_\odot$	this paper	$0.987 \pm 0.031 R_\odot$	this paper

**Fig. 1** Comparisons of masses by our method (x -axis) with the stellar masses based on spectroscopic and photometric observation (y -axis). The dashed line stands for one-to-one relationships, while the solid lines are the 3σ deviation of difference ($M_{\text{ref}} - M_{\text{model}}$). The black diamonds on the left and the right panel represent BV Dra and TW Cet, respectively.

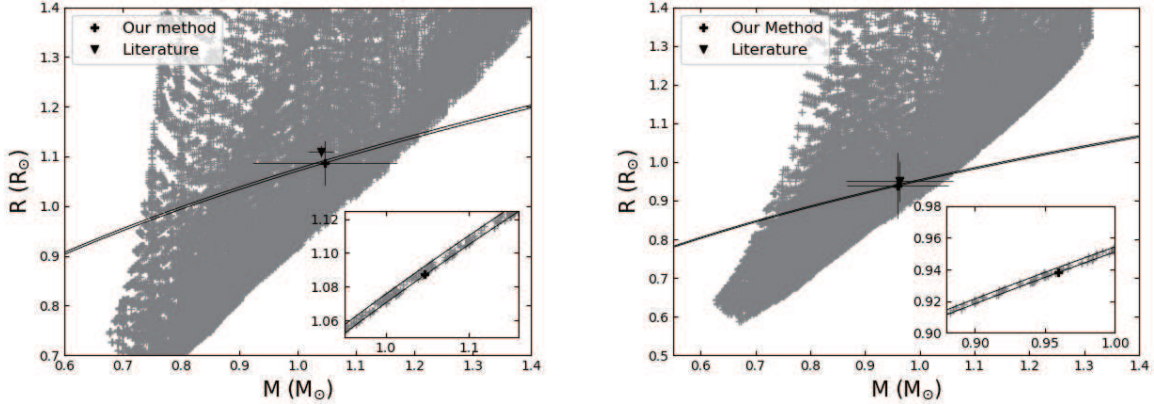


Fig. 2 The stellar M-R diagram for BV Dra (left panel) and TW Cet (right panel). The black plus marks represent the stars generated by the PARSEC evolution code, the black solid lines derive from Eq. (4). The properties from literature and estimated by our method are marked with the triangle and cross-shaped.

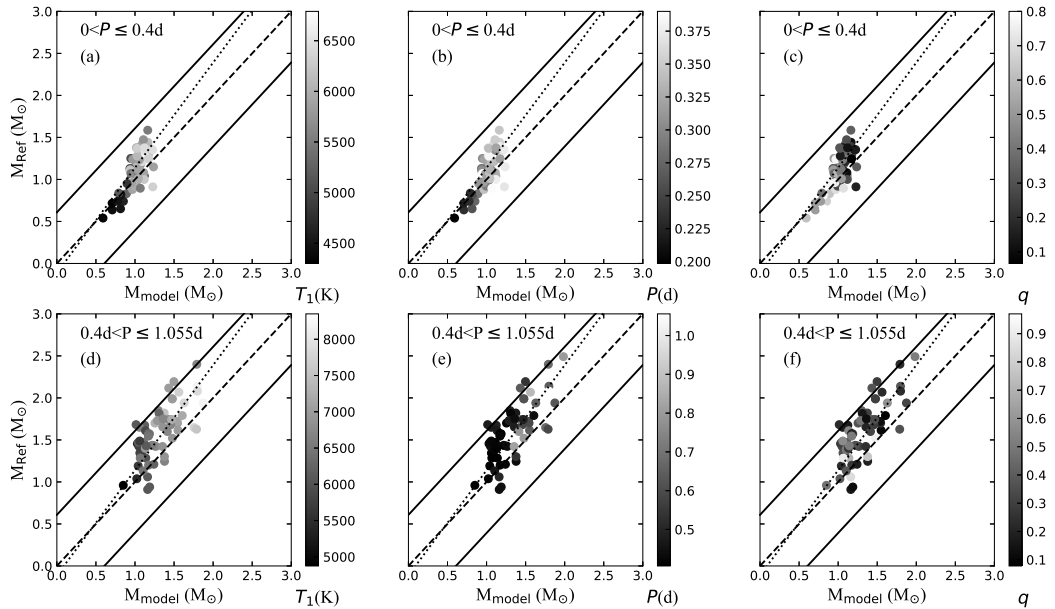


Fig. 3 The masses comparison diagram for different orbital period bins. *Upper panels*: distribution of targets with orbital period ($0 < P \leq 0.4$ d). *Bottom panels*: distribution of the rest with orbital period ($0.4d < P \leq 1.055$ d). The dashed line stands for one-to-one relationships while the solid line stands for 3σ . The dotted line represents linear fits of calculated masses and the literature values for whole targets. The different color bars represent the effective temperature of massive stars, the orbital period of systems and mass ratio, respectively.

analysis in accordance with the orbital period, the effective temperature and the mass ratio.

5.1 Orbital Period

The targets are divided into two sequences according to period, where the period shorter than 0.400 d belong to short-period sequence and the rest targets are long-period

systems (Bilir et al. 2005). The comparisons of masses for targets with different period bin are presented in Figure 3. From upper panels of this figure, we can see that the computed masses are agreement with the literature values for the targets with period shorter than 0.400 d. Besides, we discover in Figures 3(a) and (c) that the effective temperature of short-period targets ranges from 4300 K to

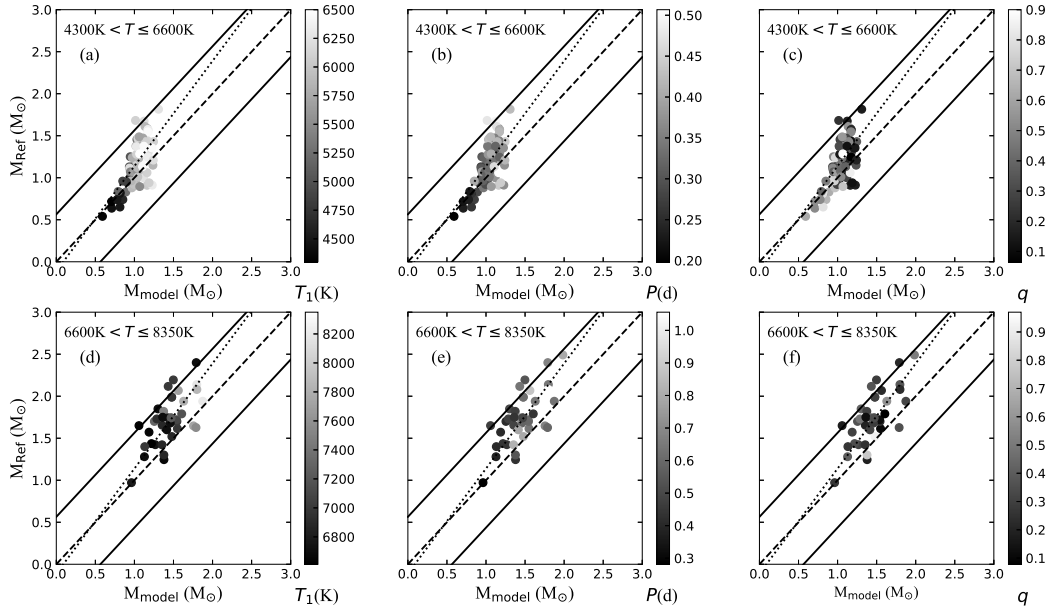


Fig. 4 Comparison diagram similar to Fig. 3. *Upper panels*: masses comparison of the low-temperature ($4300 \text{ K} \leq T_1 \leq 6600 \text{ K}$) targets. *Bottom panels*: masses comparison of high-temperature ($6600 \text{ K} < T_1 \leq 8350 \text{ K}$) targets.

6790 K, and the mass ratio ranges from 0.066 to 0.800. In the meanwhile, a variation tendency is also discovered in Figure 3(b) that the discrepancy increases as the orbit period increases. The bottom panels of Figure 3 indicate that the mass values are slightly lower than the literature values for the long-period region ($0.4 \text{ d} < P \leq 1.055 \text{ d}$).

The effective temperatures of the long-period stars cover the ranges of 5326 K–8350 K and the mass ratios vary from 0.078–0.970, respectively, as shown in Figures 3(e) and (f).

The average fractional difference and standard deviation are 12.13% and 0.1485, 18.40% and 0.2220 for short- and long-period systems, respectively. A preliminary conclusion is drawn that the method is more suitable for short-period targets in comparison to long-period targets.

5.2 Effective Temperature

According to the investigation of Qian et al. (2017), the targets are divided into two sequences based on whether the effective temperature of massive companion stars are more than 6600 K. The comparisons of masses for targets with the different effective temperature bin are presented in Figure 4. As revealed in Figure 4(a), the residuals increase with the increasing of effective temperature for low-temperature ($4300 \text{ K} \leq T_1 \leq 6600 \text{ K}$) targets. It can be found in Figure 4(b) that the orbital period is located in 0.198 d to 0.506 d interval, which adds

further support for the period-color-luminosity relation (Rucinski & Duerbeck 1997). The mass ratio lies in 0.066 to 0.900 for these low-temperature targets as shown in Figure 4(c). From Figure 4(d), we notice that the targets with high-temperature ($6600 \text{ K} < T_1 \leq 8350 \text{ K}$) exist a large discrepancy between our result and the reference masses, with no striking trends in the residuals relative to the temperature. The ranges of orbital period and mass ratio for high-temperature targets are 0.281 d to 1.055 d and 0.078 to 0.970, respectively.

The average fractional difference and standard deviation for the high- and low-temperature systems are 14.66% and 0.1880, 16.53% and 0.2196, respectively. Compared with high-temperature targets, the targets with low-temperature have a better agreement between these mass parameters from literature and that estimated by our method.

5.3 Mass Ratio

The critical mass ratio $q = 0.55$ is a peak of energy transfer rate for W UMa systems on the basis of the investigation of Li et al. (2008). Therefore, we divided the samples into two sequences according to whether the mass ratio is greater than 0.55. The distribution of our results and the references in different bins of mass ratio are plotted in Figure 5. The upper panels of this figure show that the literature values are slightly higher than those values

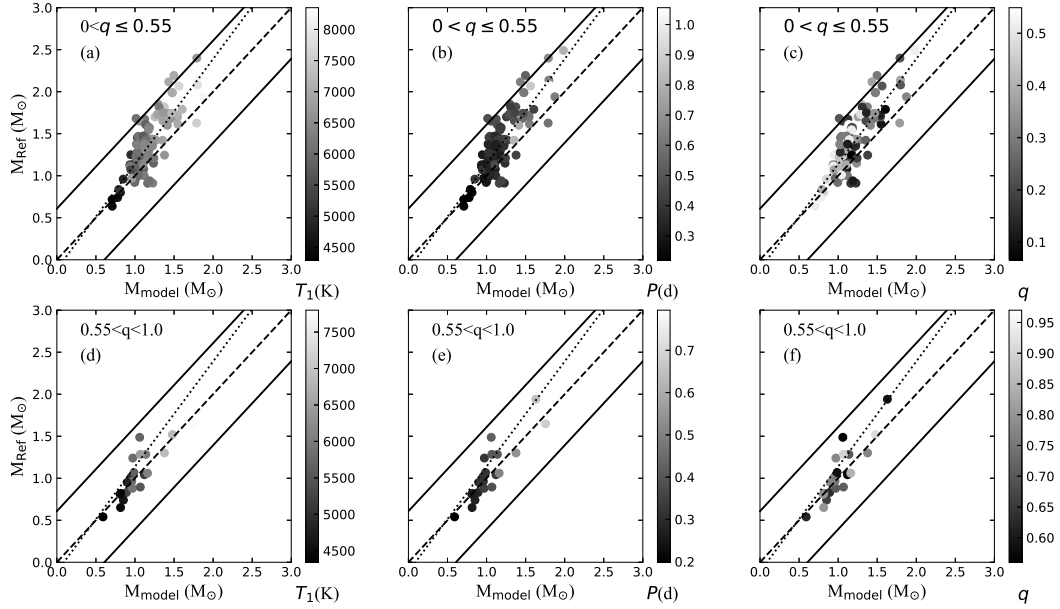


Fig. 5 Comparison diagram similar to Fig. 3. *Upper panels*: distribution of the targets with the mass ratio ($q \leq 0.55$). *Bottom panels*: distribution of the targets with mass ratio ($q > 0.55$) are presented in the lower part.

derived by our model for the targets with low mass ratio ($0 < q < 0.55$). There are just 22 targets with high mass ratio ($0.55 < q < 1.0$) as shown in bottom panels, and we can find the M_{model} values are almost consistent with those from literature.

The average fractional difference and standard deviation for the high- and low-mass ratio systems are 10.57% and 0.1559, 16.07% and 0.2026 respectively. Therefore, we suggest that the method is likely to be more applicable for those targets with larger mass ratio. However, the effect of mass ratio in our method remains to be elucidated in the future.

In addition to the above descriptions, two parts also need to be elaborated. First, the effective temperature usually is estimated based on spectral type or color index. Considering the fact that the color-temperature relation is empirical, the effective temperature decided by the color indices relation may be inaccurate. Meanwhile, [Yakut & Eggleton \(2005\)](#) demonstrated that even though all spectral types and temperatures strictly follow the well-determined relation by [Popper \(1980\)](#), it is difficult to confirm the fairly accurate effective temperature. We suggest that the effective temperature from spectral types may be more accurate than that from color indices. Second, it is admittedly that the range of accurate metallicity exists a great significance to estimate masses of W UMa binaries. In this work, we presume the metallicity range with

0.0001–0.0070 for all samples. However, the metallicity of the majority of the samples are not measured in former research. Therefore, more spectral observations with high precision are indispensable to obtain the metallicity in the future.

Acknowledgements We thank the anonymous referee for constructive comments that significantly improved the quality of the paper. This work is supported by the National Natural Science Foundation of China (No. 11661161016), the program of Tianshan Youth (No. 2017Q091), the 13th Five-year information Plan of Chinese Academy of Sciences (No. XXH1350303-107) and the Natural Science Foundation of Yunnan Province (No. 2017HC018).

References

- Ahn, Y. S., Hill, G., & Khalesseh, B. 1992, *A&A*, 265, 597
- Albayrak, B., Djurašević, G., Selam, S. O., et al. 2005, *New Astron.*, 10, 163
- Andersen, J. 1991, *A&A Rev.*, 3, 91
- Archer, S. 1959, *ApJ*, 130, 774
- Baran, A., Zola, S., Rucinski, S. M., et al. 2004, *Acta Astronomica*, 54, 195
- Barnes, J. R., Lister, T. A., Hilditch, R. W., et al. 2004, *MNRAS*, 348, 1321
- Batten, A. H., & Lu, W. 1986, *PASP*, 98, 92
- Bessell, M. S., & Brett, J. M. 1988, *PASP*, 100, 1134
- Bessell, M. S. 1990, *PASP*, 102, 1181

- Bertelli, G., Bressan, A., Chiosi, C., Fagotto, F., & Nasi, E. 1994, *A&AS*, 106, 275
- Bilir, S., Karataş, Y., Demircan, O., & Eker, Z. 2005, *MNRAS*, 357, 497
- Binnendijk, L. 1970, *Vistas in Astronomy*, 12, 217
- Borkovits, T., Elkhateeb, M. M., Csizmadia, S., et al. 2005, *A&A*, 441, 1087
- Bressan, A., Marigo, P., Girardi, L., et al. 2012, *MNRAS*, 427, 127
- Çalışkan, Ş., Latković, O., Djurašević, G., et al. 2014, *AJ*, 148, 126
- Chen, Y., Girardi, L., Bressan, A., et al. 2014, *MNRAS*, 444, 2525
- Chen, Y., Bressan, A., Girardi, L., et al. 2015, *MNRAS*, 452, 1068
- Cillié, G. G., & Bok, B. J. 1951, *AJ*, 56, 35
- Chevallard, J., & Charlot, S. 2016, *MNRAS*, 462, 1415
- Christopoulou, P.-E., Parageorgiou, A., & Chrysopoulos, I. 2011, *AJ*, 142, 99
- Csizmadia, S., & Klagyivik, P. 2004, *A&A*, 426, 1001
- Dapergolas, A., Kontizas, E., & Kontizas, M. 1989, *Information Bulletin on Variable Stars*, 3377, 1
- Davenport, J. R. A., Becker, A. C., West, A. A., et al. 2013, *ApJ*, 764, 62
- Deb, S., & Singh, H. P. 2011, *MNRAS*, 412, 1787
- Djurašević, G., Dimitrov, D., Arbutina, B., et al. 2006, *PASA*, 23, 154
- Djurašević, G., Yılmaz, M., Baştürk, Ö., et al. 2011, *A&A*, 525, A66
- Djurašević, G., Batırk, Ö., Latković, O., et al. 2013, *AJ*, 145, 80
- Duerbeck, H. W., & Rucinski, S. M. 2007, *AJ*, 133, 169
- Eggleton, P. P. 1983, *ApJ*, 268, 368
- Erdem, A., & Özkardeş, B. 2006, *New Astron.*, 12, 192
- Fu, X., Bressan, A., Marigo, P., et al. 2018, *MNRAS*, 476, 496
- Gazeas, K. D., Baran, A., Niarchos, P., et al. 2005, *Acta Astronomica*, 55, 123
- Gazeas, K. D., Niarchos, P. G., Zola, S., Kreiner, J. M., & Rucinski, S. M. 2006, *Acta Astronomica*, 56, 127
- Geyer, E. H., Hoffmann, M., & Karimie, M. T. 1982, *A&AS*, 48, 85
- Girardi, L., Dalcanton, J., Williams, B., et al. 2008, *PASP*, 120, 583
- Goecking, K.-D., & Duerbeck, H. W. 1993, *A&A*, 278, 463
- Gorda, S. Y. 1986, *Information Bulletin on Variable Stars*, 2906, 1
- Gorda, S. Y. 2016, *Astrophysical Bulletin*, 71, 64
- Gürol, B. 2005, *New Astron.*, 10, 653
- Gürol, B. 2016, *New Astron.*, 47, 57
- Gürol, B., Bradstreet, D. H., Demircan, Y., et al. 2015, *New Astron.*, 41, 26
- Gürol, B., Gökyay, G., Saral, G., et al. 2016, *New Astron.*, 46, 31
- Hardie, R. H., & Hall, D. S. 1990, *Journal of Astrophysics and Astronomy*, 11, 265
- Hilditch, R. W., King, D. J., & McFarlane, T. M. 1988, *MNRAS*, 231, 341
- Hilditch, R. W., King, D. J., & McFarlane, T. M. 1989, *MNRAS*, 237, 447
- Jayasinghe, T., Stanek, K. Z., Kochanek, C. S., et al. 2020, *MNRAS*, 491, 13
- Kähler, H. 2002, *A&A*, 395, 907
- Kalomeni, B., Yakut, K., Keskin, V., et al. 2007, *AJ*, 134, 642
- Kaluzny, J. 1984, *Acta Astronomica*, 34, 217
- Kaluzny, J., & Rucinski, S. M. 1986, *AJ*, 92, 666
- Kim, C.-H., Lee, J. W., Kim, S.-L., Han, W., & Koch, R. H. 2003, *AJ*, 125, 322
- Kjurkchieva, D. P., Marchev, D. V., & Popov, V. A. 2018, *Astronomische Nachrichten*, 339, 472
- Kjurkchieva, D. P., Popov, V. A., & Petrov, N. I. 2019a, *New Astron.*, 68, 20
- Kjurkchieva, D., Stateva, I., Popov, V. A., & Marchev, D. 2019b, *AJ*, 157, 73
- Köse, O., Kalomeni, B., Keskin, V., Ulaş, B., & Yakut, K. 2011, *Astronomische Nachrichten*, 332, 626
- Kouzuma, S. 2019, *PASJ*, 71, 21
- Kreiner, J. M., Rucinski, S. M., Zola, S., et al. 2003, *A&A*, 412, 465
- Kuiper, G. P. 1941, *ApJ*, 93, 133
- Lapasset, E., & Gomez, M. 1990, *A&A*, 231, 365
- Lee, J. W. L., Han, W., & Kim, C.-H. 1999, *Journal of Astronomy and Space Sciences*, 16, 227
- Lee, J. W., Lee, C.-U., Kim, S.-L., et al. 2011, *PASP*, 123, 34
- Lee, J. W., Youn, J.-H., Park, J.-H., & Wolf, M. 2015, *AJ*, 149, 194
- Li, K., & Qian, S.-B. 2013, *New Astron.*, 21, 46
- Li, L., Zhang, F., Han, Z., Jiang, D., & Jiang, T. 2008, *MNRAS*, 387, 97
- Li, H.-L., Wei, J.-Y., Yang, Y.-G., & Dai, H.-F. 2016, *Research in Astronomy and Astrophysics*, 16, 2
- Lister, T. A., McDermid, R. M., & Hilditch, R. W. 2000, *MNRAS*, 317, 111
- Liu, L., Qian, S.-B., Zhu, L.-Y., He, J.-J., & Li, L.-J. 2011, *AJ*, 141, 147
- Liu, L., Qian, S.-B., & Xiong, X. 2018, *MNRAS*, 474, 5199
- Liu, J., Esamdin, A., Zhang, Y., et al. 2019, *PASP*, 131, 084202
- Lohr, M. E., Norton, A. J., Gillen, E., et al. 2015, *A&A*, 578, A103
- Lu, W. 1993, *AJ*, 105, 646
- Lu, W., & Rucinski, S. M. 1999, *AJ*, 118, 515
- Lu, W., Rucinski, S. M., & Ogłozna, W. 2001, *AJ*, 122, 402
- Ma, S., Li, K., Li, Q.-C., et al. 2018, *New Astron.*, 59, 1
- Maceroni, C., & van't Veer, F. 1996, *A&A*, 311, 523
- Maíz Apellániz, J. 2006, *AJ*, 131, 1184
- Marigo, P., Girardi, L., Bressan, A., et al. 2008, *A&A*, 482, 883
- Marigo, P., Girardi, L., Bressan, A., et al. 2017, *ApJ*, 835, 77
- Mihalas, D. 1978, *San Francisco*, W. H. Freeman and Co., 1978. 650 p.,
- Mitnyan, T., Bódi, A., Szalai, T., et al. 2018, *A&A*, 612, A91

- Mochnacki, S. W. 1981, ApJ, 245, 650
- Mochnacki, S. W. 1984, ApJS, 55, 551
- Naresh Kumar, L., Sushma, D., & Vivekananda Rao, P. 2008, Bulletin of the Astronomical Society of India Proceedings, 25, 65
- Nelson, R. H., & Alton, K. B. 2019, Information Bulletin on Variable Stars, 6266, 1
- Nelson, R. H., Milone, E. F., van Leeuwen, J., et al. 1995, AJ, 110, 2400
- Niarchos, P. G., & Manimanis, V. N. 2003, A&A, 405, 263
- Özkarde, B., & Erdem, A. 2012, New Astron., 17, 143
- Paczyński, B. 1971, ARA&A, 9, 183
- Papageorgiou, A., & Christopoulou, P.-E. 2014, Contributions of the Astronomical Observatory Skalnate Pleso, 43, 468
- Popper, D. M. 1980, ARA&A, 18, 115
- Pribulla, T., Chochol, D., Rovithis-Livaniou, H., & Rovithis, P. 1999, A&A, 345, 137
- Pribulla, T., Chochol, D., Vanko, M., et al. 2002, Information Bulletin on Variable Stars, 5258, 1
- Pribulla, T., & Vanko, M. 2002, Contributions of the Astronomical Observatory Skalnate Pleso, 32, 79
- Pych, W., Rucinski, S. M., DeBond, H., et al. 2004, AJ, 127, 1712
- Qian, S., & Yang, Y. 2005, MNRAS, 356, 765
- Qian, S.-B., He, J.-J., Liu, L., et al. 2008, AJ, 136, 2493
- Qian, S.-B., Zhang, J., Wang, J.-J., et al. 2013, ApJS, 207, 22
- Qian, S.-B., He, J.-J., Zhang, J., et al. 2017, RAA (Research in Astronomy and Astrophysics), 17, 087
- Rainger, P. P., Hilditch, R. W., & Bell, S. A. 1990, MNRAS, 246, 42
- Rucinski, S. M., & Duerbeck, H. W. 1997, PASP, 109, 1340
- Rucinski, S. M., Lu, W., Mochnacki, S. W., et al. 2001, AJ, 122, 1974
- Rucinski, S. M., Lu, W., Capobianco, C. C., et al. 2002, AJ, 124, 1738
- Russo, G., Sollazzo, C., Maceroni, C., et al. 1982, A&AS, 47, 211
- Selam, S. O., Albayrak, B., Şenavci, H. V., et al. 2005, Astronomische Nachrichten, 326, 746
- Selam, S. O., Esmer, E. M., Şenavci, H. V., et al. 2018, Ap&SS, 363, 34
- Szalai, T., Kiss, L. L., Mészáros, S., Vinkó, J., & Csizmadia, S. 2007, A&A, 465, 943
- Tang, J., Bressan, A., Rosenfield, P., et al. 2014, MNRAS, 445, 4287
- Torres, G., Andersen, J., & Giménez, A. 2010, A&A Rev., 18, 67
- Wang, Y.-H., Liu, J.-Z., Lu, L.-N., et al. 2019, Research in Astronomy and Astrophysics, 19, 108
- Xiao, Z., Shengbang, Q., Binghe, H., Hao, L., & Jia, Z. 2016, PASJ, 68, 102
- Yakut, K., & Eggleton, P. P. 2005, ApJ, 629, 1055
- Yamasaki, A. 1979, Ap&SS, 60, 173
- Yang, Y., & Liu, Q. 2003a, A&A, 401, 631
- Yang, Y., & Liu, Q. 2003b, New Astron., 8, 465
- Yang, Y., & Liu, Q. 2003c, AJ, 126, 1960
- Yang, Y.-G., Qian, S.-B., & Zhu, L.-Y. 2005, AJ, 130, 2252
- Yang, Y.-G., Lü, G.-L., Yin, X.-G., Zhu, C.-H., & Nakajima, K. 2009a, AJ, 137, 236
- Yang, Y.-G., Qian, S.-B., Zhu, L.-Y., et al. 2009b, AJ, 138, 540
- Yang, Y.-G. 2012, RAA (Research in Astronomy and Astrophysics), 12, 419
- Zhu, L. Y., Qian, S. B., Liu, N. P., Liu, L., & Jiang, L. Q. 2013, AJ, 145, 39
- Zola, S., Kreiner, J. M., Zakrzewski, B., et al. 2005, Acta Astronomica, 55, 389
- Zola, S., Rucinski, S. M., Baran, A., et al. 2004, Acta Astronomica, 54, 299
- Zola, S., Gazeas, K., Kreiner, J. M., et al. 2010, MNRAS, 408, 464